

Direct Comparison Using Coulomb Counting and Open Circuit Voltage Method for the State of Health Li-Po Battery

Lora Khaula Amifia

Faculty of Electrical Technology and Intelligent Industry, Institut Teknologi Telkom Surabaya, Surabaya, Indonesia
Email: loraamifia@ittelkom-sby.ac.id

Abstract—Electric cars have undergone many developments in the current digital era. This is to avoid the use of increasingly scarce fuel. Recent studies on electric cars show that battery estimation is an interesting topic to be implemented directly. The battery estimation strategy is carried out by the Battery Management System (BMS). BMS is an indispensable part of electric vehicles or hybrid vehicles to ensure optimal and reliable operation of regulating, monitoring, and protecting batteries. A reliable BMS can extend battery life by setting voltage, temperature, and charging and discharging current limits. The main estimation strategy used by BMS is battery fault, SOH, and battery life. Battery State of Health (SOH) is part of the information provided by the BMS to avoid battery damage and failure. SOC is the proportion of battery capacity SOH is a measure of battery health. This study aims to develop a method for estimating SOH simultaneously using Coulomb Counting and Open Circuit Voltage (OCV) algorithms. The battery is modeled to obtain battery parameters and components of internal resistance, capacitance polarization and OCV voltage source. Several tests were implemented in this research by applying the constant current (CC)-charge CC-discharge test. The state-space system is then formed to apply the Coulomb Counting and OCV algorithms so that SOH can be estimated simultaneously. The OCV-SOC function is obtained in the form of a tenth order polynomial and the battery model parameters say that these parameters change with the health of the battery. The results of the model validation are able to accurately model the battery with an average relative error of 0.027%. Coulomb Counting resulted in an accurate SOH estimation with an error of 3.4%.

Keywords—State of Health (SOH); Coulomb Counting; Open Circuit Voltage (OCV)

I. INTRODUCTION

In the current era of developing technology, the high population and massive vehicles raise new problems. The research background are many vehicles fill the streets every day which can cause traffic jams, vehicle smoke continues to billow from the exhaust which emits carbon emissions and contributes significantly to air pollution and global warming [1]. With this phenomenon, a solution is needed to make the surrounding environment safer and healthier [2], [3], [4]. One solution is electric vehicles that use battery energy sources to slow down the rate of global warming. Batteries do not produce emissions like gasoline or diesel, so they can reduce pollution and reduce global warming [5]. However, the battery is not one of the cheap vehicle components so we need

a way to keep the battery having an optimal and healthy life time [6], [7].

Electric vehicle batteries have a relatively small capacity and voltage. A battery system usually consists of many cells [8]. To manage it, a battery management system (BMS) is required for state of health (SOH) estimation. SOH initially comes from SOC which cannot be measured directly so estimation is needed [9], [10], [11]. Accurate estimation will affect battery health and prevent battery from damage. SOH is a quantization of battery performance [12]. SOH estimation helps determine the actual condition of the battery after repeatedly experiencing the charge-discharge process. Batteries will experience a process of quality degradation due to use and increase in cycle [13], [14] life. This causes the parameters in the battery to change and cause a decrease in performance. One of the parameters in the battery that changes is the internal resistance of the battery. Another parameter is battery capacity. As the cycle life [15], [16] increases, the battery capacity decreases.

The battery elements, namely current, voltage, and temperature, are physical quantities that can be measured directly [17]. Meanwhile, battery capacity, battery health cannot be measured directly, so an algorithm is needed to estimate it. The related work from the past research are developed many battery estimation algorithms includes Coulomb Counting, Neural Network (NN), Fuzzy Logic, ANFIS, Open Circuit Voltage (OCV), Kalman Filter [18], [19], [20] and so on. From related research, it is stated that the simulation results of the proposed OCV model can increase the SOC of the battery compared to the casing without the model [21], [22]. In addition, the proposed model produces more aggregators for voltage and frequency regulation services. The voltage stability produced by the OCV model is also better than all network buses considered [23], [24], [25]. As for the Coulomb Counting method and open-circuit voltage calculations which can provide accurate real-time estimates of SOC. The algorithm is one method that depends on the application of the battery system and the requirements of the battery management system [26], [27]. Coulomb Counting and OCV battery parameters were obtained using the recursive least square (RLS) algorithm and were able to anticipate the nonlinear nature of the battery [28], [29]. One of the advantages of the RLS algorithm is that it is accurate in determining the parameter values for each iteration so that the parameter changes can be seen [30].



Comparative studies were also carried out on several battery models, such as the Thevenin battery model with one RC ladder which was the best considering its complexity, accuracy, and durability. Another parameter that needs to be obtained so that the battery model can be used is the OCV voltage [31]. And to get the OCV-SOC curve, it is necessary to use the terminal voltage data in the charging and discharging process [32]. When charging, the battery is connected to the charger for a few minutes then the charger is removed and the battery is allowed to rest until the voltage reaches a steady state [33]. The part of the steady voltage is sampled then the process is repeated again until the battery is full. Then the results of the voltage sample are connected so that the OCV curve is obtained when charging. Almost a similar process is carried out when discharging. The battery is connected to a load for 5 minutes then rested until it reaches a steady voltage [34], [35], [36]. The test is then called a pulse test. From the steady test conditions, the OCV discharging curve can be obtained. The two curves are then positioned at the same SOC and then averaged [37], [38]. The result is an OCV-SOC curve and with curve fitting we can get the equation in polynomial form. Another method that is almost similar to obtain the OCV-SOC function is by averaging the terminal voltage from the constant current method of charging with the discharging terminal voltage of the constant current method at the same SOC. Curve fitting is used to get the equation of function.

The measure of battery health can be seen from changes in capacity, internal resistance or other parameters as the number of battery life cycles increases [39]. In this study, the Thevenin battery model is used which is the best choice in terms of accuracy, complexity, and durability. SOH estimation methods used in this study are Coulomb Counting and OCV. An important part of a battery model is finding the right parameters in it. The innovation of this research is by applying a battery model that has a lighter dynamic parameter value, namely the polarized resistance and capacitance parameters. The Thevenin model consists of one OCV source voltage, one internal resistance, and one parallel section containing polarizing resistance and polarizing capacitance. And other parameters have been identified with the recursive least square (RLS) algorithm, because of its recursive ability which allows the latest parameters to be obtained in each iteration so that the parameter characteristics can be obtained accurately. The main research contribution is to make the battery in a healthy condition so that it can extend battery life, help and understand alternative SOH estimation methods, and reduce the computational burden on the BMS.

II. METHOD

BMS is an indispensable part of electric vehicles or hybrid vehicles to ensure optimal and reliable operation of regulating, monitoring, and protecting batteries [40], [41] (Fig. 1). BMS aims to extend battery life by determining the limits for voltage, temperature, SOC, and SOH and limits for charging and discharging currents. The main estimation strategies used by BMS are battery fault, SOC, SOH, and battery life. SOC and SOH is an important part to maintain the condition of the battery [42]. Proper SOC estimation can prevent the battery from overcharge and over-discharge.

While the SOH can find out the proper condition of using the battery.

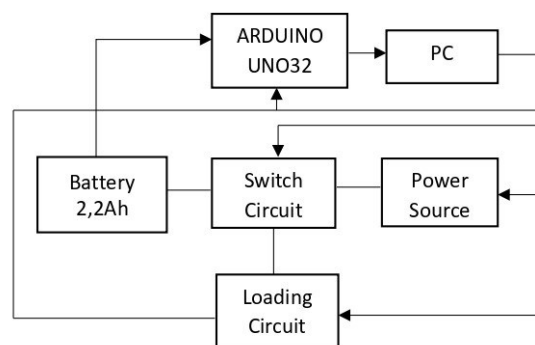


Fig. 1. Experimental Design

A. Battery

The battery used in this study is a Lithium Polymer battery. This battery consists of three cells but in this study only one battery cell was used. The battery has a capacity of 2200mAh, with a maximum discharge current of 44A and a maximum charge rate of current of 4.4A.

B. LiPo Balance Charger iMAX B6

This charger has several capabilities. One of the capabilities used in this research is charging with the constant current-constant voltage (CC-CV) method. This capability allows the battery to be fully charged. The CC-CV process starts from the condition that the battery runs out or has been used [43]. The battery will be charged in CC mode with a constant current until the battery voltage reaches the maximum limit and in this study is 4.2 Volts. After that, the charger will change the mode to CV with the charger current will gradually decrease until the battery is completely full. This method attempts to keep the battery healthy.

C. Dummy Load

A dummy load is a device used to simulate electrical loads, usually for testing purposes. In this study, a dummy load branded GWINSTEK PEL-2004 was used. PEL-2004 has several modes such as constant current, constant voltage, constant resistance, constant power, and sequence.

D. Current Regulator LM317

This circuit is used to provide a constant current input to the battery of ± 2.2 A (Fig. 2 and Fig. 3). This circuit is used because the iMAX B6 charger will die if the battery is disconnected from the charger when used in a switching circuit. In practice, the value of $R_1 = 2.2$ is used and the four circuits are arranged in parallel to obtain a current of 2.159 A.

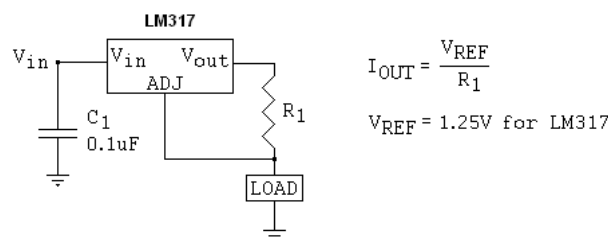


Fig. 2. Current Regulator LM 317

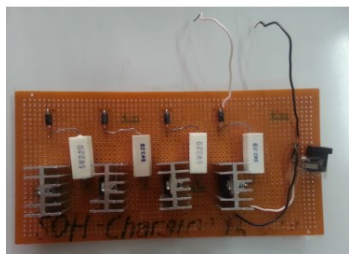


Fig. 3. Charger LM317

E. Loading Circuit

This circuit is connected to the battery, charger, dummy load, and Arduino UNO32. This circuit serves to regulate when the battery is connected to the charger, the load, or not connected to both. In this circuit there is also a current sensor and a voltage sensor [44].

F. Arduino UNO32

In this research, Arduino is used to control the switching process. In addition, Arduino is also used to record current and voltage sensor data. The recorded data will be entered into a personal computer to store battery current and voltage data using Microsoft Excel. Through a PC, MATLAB is used to process the data. Likewise in the development of estimation algorithms. In addition, the program for data retrieval via Arduino also starts from MATLAB.

G. System Design

Fig. 4 is a block diagram of the entire system containing many parts, including the most important part, namely the implementation of the Coulomb Counting and OCV methods.

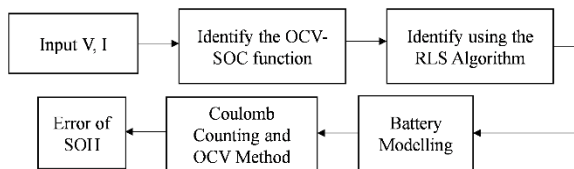


Fig. 4. Block Diagram Coulomb Counting OCV System

From the block diagram in Fig. 4, it is described step by step as follows.

- *Battery input (V, I)*

Input is taken directly from two important elements of the battery, namely voltage (V) and current (I) which is then taken data to identify parameters.

- *Data processing*

Tests the battery with various inputs and records the output. Various kinds of tests were carried out to support the development of the SOH estimation algorithm. Tests were also carried out to validate the research results.

- *Identify the Function of OCV-SOC*

Get battery OCV-SOC function. It is useful in battery modeling. In addition, this function is also used to estimate SOH through the Coulomb Counting. The OCV-SOC function relates to battery modeling accuracy [45]. And to get the battery model parameters with the RLS algorithm. The algorithm is implemented by inputting the battery test voltage

and current data. The algorithm output is the battery model parameter.

- *Identify Battery Parameters*

Getting the battery model parameters with the RLS algorithm. The algorithm is implemented by inputting the battery test voltage and current data. The algorithm outputs are parameters R_0 , R_p , and C_p of the battery model.

- *Battery Modelling*

After obtaining the parameters, the battery model is run and validated by providing current input to the model. The model output voltage is compared with the test data voltage. If the model error is more than 1%, improve the RLS algorithm, if the error is less than 1%, proceed to the next step.

- *Estimation of SOH*

After obtaining the parameters, the battery model is run and validated by providing current input to the model. The model output voltage is compared with the test data voltage. If the model error is more than 1%, improve the RLS algorithm, if the error is less than 1%, proceed to the next step. Developed an algorithm for SOH estimation. If the estimation results are not running, correct and develop the system again until good results are obtained. The results obtained from the development of the algorithm are analyzed and written into a scientific report.

III. STATE OF HEALTH EXPERIMENT

A. Static Capacity Test

Static capacity test is useful for knowing battery capacity in ampere hours with constant current [46], [47]. This test is carried out by placing a load on the battery so that the battery produces a constant current until it reaches the voltage limit stated on the battery product [48]. If it is not stated, then 50% of the maximum battery voltage is used as the discharge limit. A test with a current of 1C is commonly used in this test.

The test begins by charging the battery to its maximum voltage, on a Li-Po battery, which is 4.2 V. Then the battery is rested for one hour so that the voltage is steady and then the terminal voltage is measured at 100% SOC. The terminal voltage at that time also shows the OCV voltage because the battery is not connected to the load. After that, the battery is discharged with a current of 1C for one hour to get the actual capacity value and get the battery voltage limit or 0% SOC.

Fig. 5 is a flowchart of parameter identification in battery modeling which contains several polarized resistance and capacitance parameters.

The battery is given a load so that it produces an electric current in the form of a discharging current pulse. The pulse is to reduce battery capacity little by little. In addition, it is also to sample the terminal voltage of each current worth 0 A or not connected to the load in order to get the battery V_{oc} value. The battery terminal voltage response is recorded. These data are used to identify the OCV-SOC function and parameters R_0 , R_p , and C_p . These data are also used for validation by comparing the output terminal voltages of the battery model. From the pulse test terminal voltage data, just

before the current pulse enters the battery, the terminal voltage is sampled. The sampling points of each voltage pulse are connected so that they become a voltage line V_{oc} with respect to time. By changing the time domain to the SOC domain, the voltage line V_{oc} to SOC is obtained. By applying curve fitting, the OCV-SOC function will be obtained.

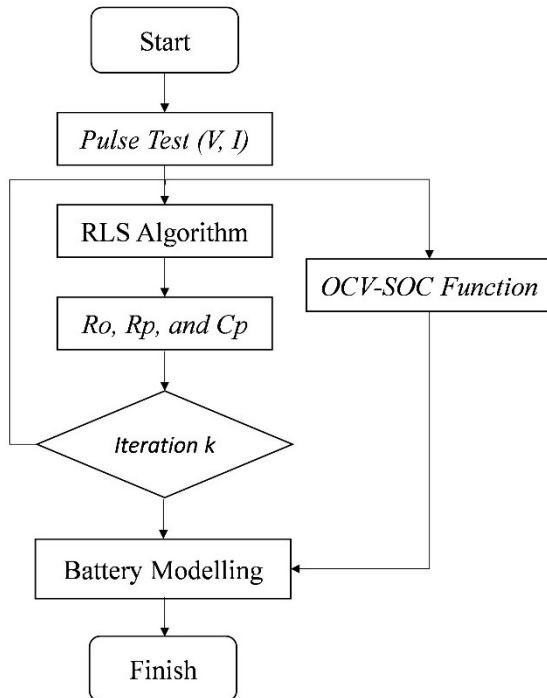


Fig. 5. Parameter Identification on Battery Modelling

The RLS algorithm is to provide input in the form of current and voltage pulse test. It is carried out by providing input in the form of current and pulse test voltage [49]. The relationship between input current and output voltage on the battery is a parameter obtained from the polarized resistance and capacitance parameter values. Parameters of R_o , R_p , C_p that can be recorded and stored. To get the dynamics of the battery model parameters, the parameter identification process is repeated until the battery SOC reaches 0%. The battery model parameters and the OCV-SOC function that have been obtained are applied to the Thevenin battery model [50], [51]. The pulse test current input is fed into the battery model to see the output voltage response of the terminals. Then it will proceed to decision making.

B. Pulse Test

Pulse test (Fig. 6) aims to obtain the OCV-SOC curve and vice versa SOC-OCV. This test needs to be done to get the V_{oc} function in a series of battery models. In addition, this test is also carried out to obtain battery parameter values. The test is carried out by discharging for 30 seconds with a current of 1C then rest for 30 seconds repeatedly until the battery voltage reaches the discharge limit. The discharging period of 30 seconds was chosen to narrow the distance between OCV samples so that the curve obtained is more accurate. Rest 30 seconds was chosen because the battery terminal voltage does not change significantly when it is greater than that. In other words, at 30 seconds the battery voltage has reached steady state.

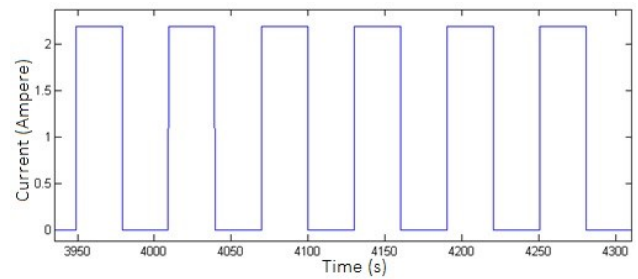


Fig. 6. Pulse test input profile

C. Pulse Variation Test

After obtaining the OCV-SOC function, parameters R_o , R_p , C_p , a test is needed to validate the battery model used. Pulse variation test (Table 1) is used for the validation process. In this test, the battery is loaded with varying currents. The current is also used as input to the battery model. The battery voltage response and the output voltage of the battery model were compared to validate the model [52]. The pulse variation test profile is based on the Dynamic Stress Test (DST). DST is one of the tests for the endurance of the battery discharge process with various load profiles [53]. One 360 second DST period with multiple discharging and charging profiles. In this study, because the LM317 charger used is only capable of producing 1C current, and the iMAX B6 charger cannot be integrated into the circuit, the charging profile on DST is removed and replaced with a rest state.

TABLE I. PULSE VARIATION TEST

Step to	Duration (second)	Discharge Current (Ampere)	Step to	Duration (second)	Discharge Current (Ampere)
1	16	0	11	12	1.1
2	28	0.55	12	8	0
3	12	1.1	13	16	0
4	8	0	14	36	0.55
5	16	0	15	6	4.4
6	24	0.55	16	24	2.75
7	12	1.1	17	8	0
8	8	0	18	32	1.1
9	16	0	19	8	0
10	24	0.55	20	44	0

D. CC-Charge and CC-Discharge Test

This test (Fig. 7) is also known as the aging cycle test, in which the battery is charged with constant current until it is full, then given a rest, then discharging with constant current and ending with rest in one period. One period of this test is referred to as one cycle life. This test is repeated with the aim of increasing the cycle life of the battery. Of course, this test will take a long time to see the effect on the battery. This test is also useful to see the SOH of the battery.

In this study, 60 charge-discharge cycles were tested. However, due to lack of tools and time, the testing process was carried out continuously for five cycles and then stopped. In the process, the battery is charged until it reaches 80% SOC then rests for 10 minutes. After that the battery is discharging to 20% SOC then rest 10 minutes. The process is repeated. Rest time is 10 minutes because at that time the battery voltage has reached steady-state.

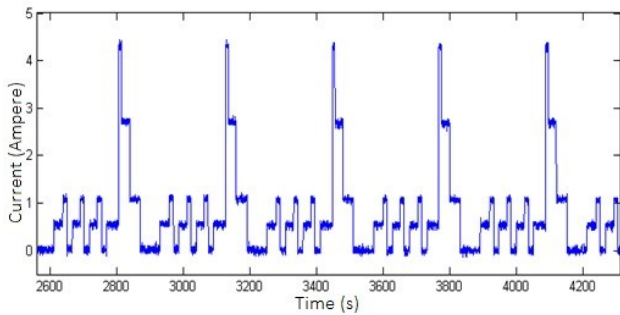


Fig. 7. Current input cutout pulse variation test

IV. STATE OF HEALTH ESTIMATION

As use and age, batteries experience a decrease in performance which is often called degradation. The degradation of battery cells affects changes in parameters in the battery such as internal resistance, capacity, electrode quality [54] and so on. The change in performance is expressed by the state of health (SOH) but universally, there is no single definition of SOH itself. SOH can also be described as the current battery performance compared to the ideal condition when the battery was new [55]. In addition, SOH can also be interpreted as a measure of the size of the current battery condition compared to its ideal condition [12], [56], [57]. The SOH unit is a percent, and 100% indicates the SOH of a new battery.

A. Battery Modelling

A Battery modeling is the key to successful determination of SOC or SOH. Battery modeling is useful for changing input battery parameters in the form of voltage, current, and temperature into SOC, SOH or various other purposes [58]. In order to estimate SOC or SOH accurately, the right battery model is needed. The Thevenin model (Fig. 8) is the best choice considering complexity, accuracy and robustness [59], [60]. I_{batt} current is the current in or out of the battery and acts as an input variable. The source voltage V_{oc} is the open circuit voltage. The terminal voltage V_t becomes the output variable. Resistance R_0 represents the internal resistance of the battery. The internal resistance of the battery consists of the resistance of the electrode material, electrolyte, separation material, and contact resistance between parts [61]. Resistance and capacitance represent the polarization resistance and capacitance which are associated with changes in the value of the voltage immediately after a voltage drop occurs or to represent the voltage transient response. This is to describe the polarization of the electrochemical process, be it concentration polarization or electrochemical polarization.

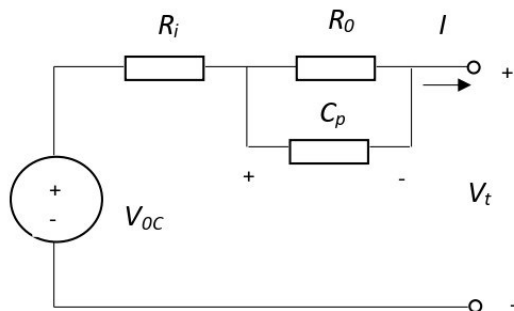


Fig. 8. Thevenin battery modelling

The mathematical equation for the battery model is as follows:

$$\dot{u}_p = -\frac{u_p}{C_p R_p} + \frac{I_{batt}}{C_p} \quad (1)$$

$$V_t = V_{oc} - u_p - I_{batt} R_0 \quad (2)$$

where u_p is the voltage across the parallel RC section.

To use the Thevenin battery model, the parameters V_{oc} , R_0 , R_p , and C_p must be identified first. Parameter identification details are as follows:

- 1) The value of V_{oc} is determined from the measurement of the terminal voltage when it is open and in steady-state.
- 2) The internal resistance R_0 is proportional to the instantaneous voltage drop, the polarization resistance and capacitance (R_p and C_p) correspond to the transient portion of the terminal voltage as the battery current changes. The mathematical equations of Thevenin battery model circuit in the frequency domain are,

$$V_t(s) - V_{oc}(s) = -I_{batt}(s) \left(R_0 + \frac{R_p}{1 + sR_p C_p} \right) \quad (3)$$

- 3) If V is $V_t - V_{oc}$, the transfer function $G(s)$, then the equation can be written as

$$G(s) = \frac{V(s)}{I_{batt}(s)} = -R_0 - \frac{R_p}{1 + sR_p C_p} \quad (4)$$

- 4) Bilinear transformation is used to convert equation (4) to discrete form by substituting,

$$s = \frac{2}{T} \frac{1 - z^{-1}}{1 + z^{-1}} \quad (5)$$

Battery modeling is done to see the error of the battery model with the actual battery. This is done in order to get an accurate system [62], [63]. The battery model parameters are used in Coulomb Counting as system equations and process equations. Because of this, the parameter values in the battery model are also used in the OCV method. Before Coulomb Counting is executed, the system state value is initialized. In the estimation of SOH, the initial value of SOH must be given first.

B. Result of SOH

SOH is obtained by looking at changes in the parameters of the battery. One parameter that changes over time and usage is capacity. By looking at the change in capacity, SOH is defined as

$$SOH_C = \frac{C_{act}}{C_{cap}} \times 100\% \quad (6)$$

Equation (6) shows where SOH_C is the SOH value, C_{act} capacity is the current maximum capacity of the battery. In general, if the battery capacity is less than 80% of the initial capacity, which means the SOH is less than 80%, then the BMS will warn the operator to replace the battery. Another parameter that changes in the degradation process is the internal resistance of the battery. The battery's internal resistance will increase in value with time and use. The

increased internal resistance causes the change in voltage when the battery is connected to a large load. It accelerates the battery to reach the terminal voltage when the battery capacity is depleted. When SOH is 100%, the internal resistance of the battery is $R_o = R_i$ where R_i is the initial internal resistance when the battery is new. When SOH is 0%, the internal resistance of the battery will change to $R_o = 2R_i$ [47]. SOH based on internal resistance can be formulated as:

$$SOH_{R_i} = \left(1 + \frac{R_i - R_o}{R_i}\right) \times 100\% \quad (7)$$

where SOH_{R_i} represents the SOH value, resistance R_i is the new battery's internal resistance, and R_o is the current internal resistance.

Fig. 9 shows the results of the static capacity test. After the battery is discharged for one hour with a constant current of 1C, the character of the battery voltage can be seen from 100% SOC to 0% SOC conditions. When the discharge time is more than 3000 seconds or SOC 20%, the battery voltage changes drastically. This is one proof that the battery is a nonlinear system. From the test, the discharging terminal voltage value is 1C SOC 100% = 4.20 volts, SOC 80% = 3.93 volts, SOC 20% = 3.63 volts and SOC 0% = 1.98 volts. The terminal voltages when SOC 80% and 20% are used for limits on CC-charge and CC-discharge tests to prevent the battery from overcharge and over-discharge.

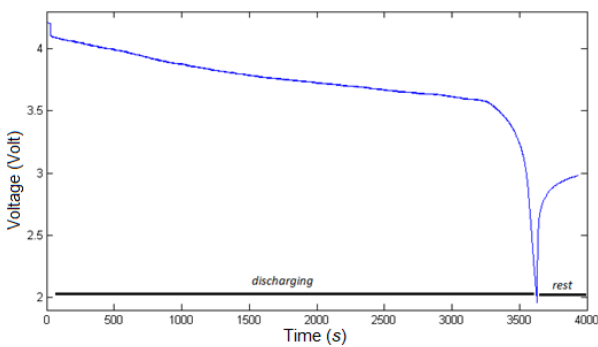


Fig. 9. Static Capacity Test

The open circuit voltage OCV(SOC) is required as the source voltage in the Thevenin battery model. The OCV is obtained from the pulse test as shown in Figure 10. When resting on the pulse test, the battery voltage is not connected to the load. The voltage just before connecting the load is sampled for each pulse and connected until the red OCV is obtained in Fig. 10.

Battery usage is easier and more precisely expressed in SOC. Therefore, the estimated OCV of the pulse test is made into a function of SOC. The red line in the Fig. 11 is the result of fitting the OCV estimate.

Fig. 12 shows the internal resistance data measured and estimated using RLS and Coulomb Counting. There was a spike in data decline four times. When the battery is drawn current, the battery voltage that is read by the sensor does not increase immediately. This is because the sampling period of the voltage sensor is less small so it is less able to read large changes in a short time in battery voltage.

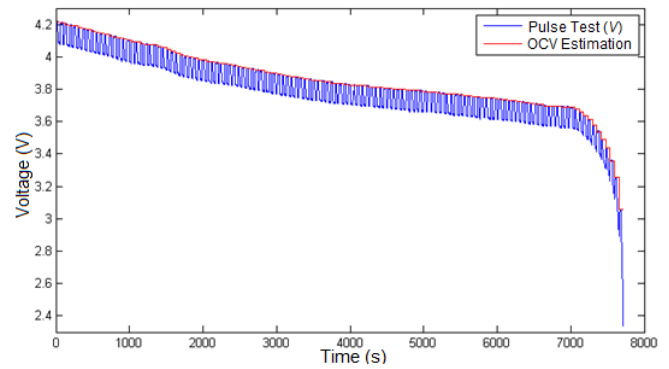


Fig. 10. Pulse Test Voltage

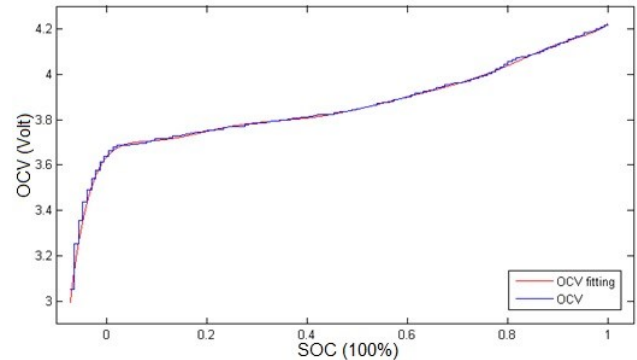


Fig. 11. Curve fitting OCV-SOC function

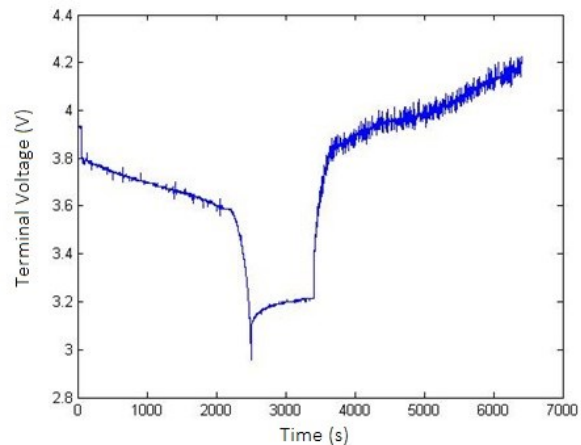


Fig. 12. OCV estimation with the RLS algorithm

Fig. 13 shows the estimation of SOH using OCV and the RLS algorithm with the measurement results. The internal resistance of OCV has a value that is not much different from RLS. This is indicated by the relative error of the two algorithms. In the OCV method, the average relative error of the estimated R_0 is 11%, while with the RLS algorithm the relative error is 10%. In estimation for one battery cycle by pulse test, the RLS algorithm is more accurate than CC.

Fig. 14 shows the estimated capacity of the battery during the pulse test. The pulse test was carried out on a new battery so that the battery capacity was still 2.2 Ah. The fluctuations that occur are also still in the range of 2.2 Ah, so the situation is constant.

From the SOC test, the internal resistance, and the battery capacity, it can be concluded that the estimation results of the

Coulomb Counting are accurate. However, the OCV has not shown the ability to estimate SOH in more than one discharge data. CC-discharge and CC-charge data are used to test the estimated SOH of the battery by looking at changes in internal resistance and battery capacity.

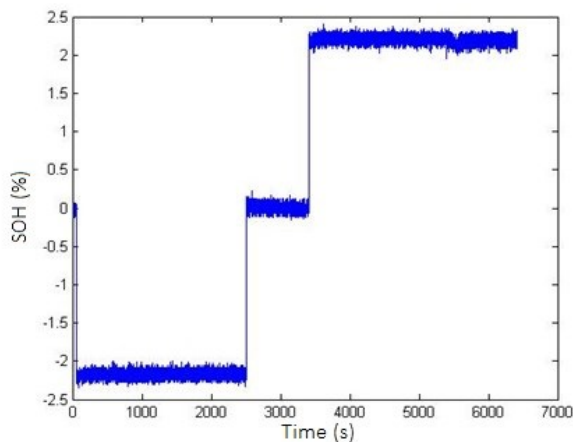


Fig. 13. SOH estimation using Open Circuit Voltage

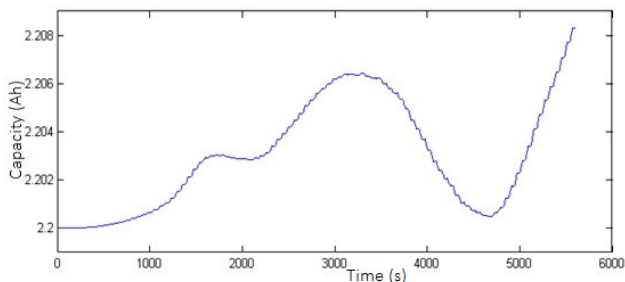


Fig. 14. Estimated battery capacity

For the estimation of SOH, two pieces of data are used. The data is the CC-Charge and CC-Discharge test data for 6 cycles. Main findings of the present study are the Coulomb Counting succeeded in estimating the terminal voltages V_t , SOC and SOH of the battery simultaneously. The estimation errors of V_t and SOC are 0.13% and 0.4%. The third data is 60 charging-discharging cycles. In this test, the SOH estimation is compared with the RLS algorithm with Coulomb Counting. The results show Coulomb Counting has better accuracy than OCV. The estimation error with Coulomb Counting is 3.4% while the OCV is 7.08%. In addition, it was also found that Coulomb Counting was able to estimate the terminal voltage and SOC of the battery while OCV was only able to estimate the battery parameters. The model validation is able to accurately model the battery with an average relative error of 0.027%.

CONCLUSION

Based on the research conducted and the results obtained that the Thevenin battery model is able to accurately model the battery with an error of 0.4% and the identification of battery parameters with the recursive least square (RLS) algorithm shows battery parameters that change with SOC, as well as estimation of SOH using the Coulomb Counting method. and accurate OCV, as evidenced by an error of 3.4%.

ACKNOWLEDGMENT

The author would like to thank the editors and reviewers for suggestions and comments to improve the quality of good and useful writing. This research was supported by Lembaga Penelitian dan Pengabdian Institut Teknologi Telkom Surabaya.

REFERENCES

- [1] K. Ranasinghe *et al.*, "Advances in Integrated System Health Management for mission-essential and safety-critical aerospace applications," *Prog. Aerosp. Sci.*, vol. 128, no. September 2021, p. 100758, 2022, doi: 10.1016/j.paerosci.2021.100758.
- [2] Z. Gong *et al.*, "Distributed Control of Active Cell Balancing and Low-Voltage Bus Regulation in Electric Vehicles Using Hierarchical Model-Predictive Control," *IEEE Trans. Ind. Electron.*, vol. 67, no. 12, pp. 10464–10473, 2020, doi: 10.1109/TIE.2019.2956396.
- [3] Y. Shang, C. Zhu, Y. Fu, and C. C. Mi, "An Integrated Heater Equalizer for Lithium-Ion Batteries of Electric Vehicles," *IEEE Trans. Ind. Electron.*, vol. 66, no. 6, pp. 4398–4405, 2019, doi: 10.1109/TIE.2018.2863187.
- [4] X. Kuang *et al.*, "Research on Control Strategy for a Battery Thermal Management System for Electric Vehicles Based on Secondary Loop Cooling," *IEEE Access*, vol. 8, pp. 73475–73493, 2020, doi: 10.1109/ACCESS.2020.2986814.
- [5] M. Mussi, L. Pellegrino, M. Restelli, and F. Trovò, "A voltage dynamic-based state of charge estimation method for batteries storage systems," *J. Energy Storage*, vol. 44, no. September, 2021, doi: 10.1016/j.est.2021.103309.
- [6] M. Corno and G. Pozzato, "Active adaptive battery aging management for electric vehicles," *IEEE Trans. Veh. Technol.*, vol. 69, no. 1, pp. 258–269, 2020, doi: 10.1109/TVT.2019.2940033.
- [7] S. M. Qaisar and M. Alqathanii, "Event-driven sampling based li-ion batteries SoH estimation in the 5G framework," *Procedia Comput. Sci.*, vol. 182, pp. 109–114, 2021, doi: 10.1016/j.procs.2021.02.015.
- [8] S. Dey, Y. Shi, K. Smith, A. Colclasure, and X. Li, "From Battery Cell to Electrodes: Real-Time Estimation of Charge and Health of Individual Battery Electrodes," *IEEE Trans. Ind. Electron.*, vol. 67, no. 3, pp. 2167–2175, 2020, doi: 10.1109/TIE.2019.2907514.
- [9] W. Liu and Y. Xu, "A Comprehensive Review of Health Indicators of Li-ion Battery for Online State of Health Estimation," *2019 3rd IEEE Conf. Energy Internet Energy Syst. Integr. Ubiquitous Energy Netw. Connect. Everything, EI2 2019*, pp. 1203–1208, 2019, doi: 10.1109/EI247390.2019.9062037.
- [10] N. Khan, F. U. M. Ullah, Afnan, A. Ullah, M. Y. Lee, and S. W. Baik, "Batteries State of Health Estimation via Efficient Neural Networks with Multiple Channel Charging Profiles," *IEEE Access*, vol. 9, pp. 7797–7813, 2021, doi: 10.1109/ACCESS.2020.3047732.
- [11] N. Chen, P. Zhang, J. Dai, and W. Gui, "Estimating the State-of-Charge of Lithium-Ion Battery Using an H-Infinity Observer Based on Electrochemical Impedance Model," *IEEE Access*, vol. 8, pp. 26872–26884, 2020, doi: 10.1109/ACCESS.2020.2971002.
- [12] S. Rahimifard, R. Ahmed, and S. Habibi, "Interacting Multiple Model Strategy for Electric Vehicle Batteries State of Charge/Health/ Power Estimation," *IEEE Access*, vol. 9, pp. 109875–109888, 2021, doi: 10.1109/ACCESS.2021.3102607.
- [13] J. H. Lee, H. S. Kim, and I. S. Lee, "State of charge estimation and state of health diagnostic method using multilayer neural networks," *2021 Int. Conf. Electron. Information, Commun. ICEIC 2021*, pp. 15–18, 2021, doi: 10.1109/ICEIC51217.2021.9369782.
- [14] S. Chowdhury, M. N. Bin Shaheed, and Y. Sozer, "An integrated state of health (SOH) balancing method for lithium-ion battery cells," *2019 IEEE Energy Convers. Congr. Expo. ECCE 2019*, pp. 5759–5763, 2019, doi: 10.1109/ECCE.2019.8912932.
- [15] M. Park, M. Seo, Y. Song, and S. Kim, "Capacity Estimation of Li-ion battery using Constant Current Charging Voltage," *Proc. - APCCAS 2019 2019 IEEE Asia Pacific Conf. Circuits Syst. Innov. CAS Towar. Sustain. Energy Technol. Disrupt.*, pp. 202–204, 2019, doi: 10.1109/APCCAS47518.2019.8953137.
- [16] S. Kulkarni, N. Walavalkar, V. Chhatre, P. Singh, and P. Sharma, "Review of optimization of charge on VRLA battery and lithium ion battery operated bike," *2020 Int. Conf. Conver. to Digit. World - Quo Vadis, ICCDW 2020*, no. Iccdw, 2020, doi: 10.1109/ICCDW45521.2020.9318678.
- [17] Z. Xia and J. A. Abu Qahouq, "Ageing characterization data of

- lithium-ion battery with highly deteriorated state and wide range of state-of-health," *Data Br.*, vol. 40, p. 107727, 2022, doi: 10.1016/j.dib.2021.107727.
- [18] D. N. T. How, M. A. Hannan, M. S. Hossain Lipu, and P. J. Ker, "State of Charge Estimation for Lithium-Ion Batteries Using Model-Based and Data-Driven Methods: A Review," *IEEE Access*, vol. 7, pp. 136116–136136, 2019, doi: 10.1109/ACCESS.2019.2942213.
- [19] J. Kuchly *et al.*, "Li-ion battery SOC estimation method using a neural network trained with data generated by a P2D model," *IFAC-PapersOnLine*, vol. 54, no. 10, pp. 336–343, 2021, doi: 10.1016/j.ifacol.2021.10.185.
- [20] M. Park, M. Seo, Y. Song, and S. W. Kim, "Capacity Estimation of Li-Ion Batteries Using Constant Current Charging Voltage with Multilayer Perceptron," *IEEE Access*, vol. 8, pp. 180762–180772, 2020, doi: 10.1109/ACCESS.2020.3028095.
- [21] I. O. Essiet and Y. Sun, "Optimal open-circuit voltage (OCV) model for improved electric vehicle battery state-of-charge in V2G services," *Energy Reports*, vol. 7, pp. 4348–4359, 2021, doi: 10.1016/j.egy.2021.07.029.
- [22] C. Chen, R. Xiong, R. Yang, and H. Li, "A Novel Operational Data-Driven Battery Open-Circuit Voltage Characterization mining method for Large-Scale Applications," *Green Energy Intell. Transp.*, vol. 1, no. 1, p. 100001, 2022, doi: 10.1016/j.geits.2022.100001.
- [23] J. Schmitt, M. Schindler, A. Oberbauer, and A. Jossen, "Determination of degradation modes of lithium-ion batteries considering aging-induced changes in the half-cell open-circuit potential curve of silicon-graphite," *J. Power Sources*, vol. 532, no. February, p. 231296, 2022, doi: 10.1016/j.jpowsour.2022.231296.
- [24] M. S. Ahmed, B. Balasingam, and K. R. Pattipati, "Experimental data on open circuit voltage characterization for Li-ion batteries," *Data Br.*, vol. 36, p. 107071, 2021, doi: 10.1016/j.dib.2021.107071.
- [25] H. Rouhi, E. Karola, R. Serna-Guerrero, and A. Santasalo-Aarnio, "Voltage behavior in lithium-ion batteries after electrochemical discharge and its implications on the safety of recycling processes," *J. Energy Storage*, vol. 35, p. 102323, 2021, doi: 10.1016/j.est.2021.102323.
- [26] S. M. Qaisar, "Event-driven approach for an efficient coulomb counting based li-ion battery state of charge estimation," *Procedia Comput. Sci.*, vol. 168, no. 2019, pp. 202–209, 2020, doi: 10.1016/j.procs.2020.02.268.
- [27] C. Stolze, P. Rohland, K. Zub, O. Nolte, M. D. Hager, and U. S. Schubert, "A low-cost amperometric sensor for the combined state-of-charge, capacity, and state-of-health monitoring of redox flow battery electrolytes," *Energy Convers. Manag. X*, vol. 14, no. January, p. 100188, 2022, doi: 10.1016/j.ecmx.2022.100188.
- [28] K. Sarrafan, K. M. Muttaqi, and D. Sutanto, "Real-Time Estimation of Model Parameters and State-of-Charge of Li-Ion Batteries in Electric Vehicles Using a New Mixed Estimation Model," *IEEE Trans. Ind. Appl.*, vol. 56, no. 5, pp. 5417–5428, 2020, doi: 10.1109/TIA.2020.3002977.
- [29] Q. Ouyang, J. Chen, and J. Zheng, "State-of-Charge Observer Design for Batteries with Online Model Parameter Identification: A Robust Approach," *IEEE Trans. Power Electron.*, vol. 35, no. 6, pp. 5820–5831, 2020, doi: 10.1109/TPEL.2019.2948253.
- [30] S. Rahimifard, S. Habibi, and J. Tjong, "Dual estimation strategy for new and aged electric vehicles batteries," *2020 IEEE Transp. Electr. Conf. Expo, ITEC 2020*, pp. 579–583, 2020, doi: 10.1109/ITEC48692.2020.9161556.
- [31] C. Xu, M. Doosthosseini, and H. K. Fathy, "Lithium-Sulfur Battery Discharge Optimization using a Thermally-Coupled Equivalent Circuit Model," *IFAC-PapersOnLine*, vol. 54, no. 20, pp. 399–405, 2021, doi: 10.1016/j.ifacol.2021.11.206.
- [32] Z. Geng, S. Wang, M. J. Lacey, D. Brandell, and T. Thiringer, "Bridging physics-based and equivalent circuit models for lithium-ion batteries," *Electrochim. Acta*, vol. 372, p. 137829, 2021, doi: 10.1016/j.electacta.2021.137829.
- [33] Z. A. Arfeen, M. P. Abdullah, U. U. Sheikh, A. Hamza Sule, H. T. Alqali, and R. Kolawole Soremekun, "Rule-based enhanced energy management scheme for electric vehicles fast-charging workplace using battery stacks and solar power," *PECon 2020 - 2020 IEEE Int. Conf. Power Energy*, pp. 113–118, 2020, doi: 10.1109/PECon48942.2020.9314614.
- [34] D. Rosewater, R. Baldick, and S. Santoso, "Risk-Averse Model Predictive Control Design for Battery Energy Storage Systems," *IEEE Trans. Smart Grid*, vol. 11, no. 3, pp. 2014–2022, 2020, doi: 10.1109/TSG.2019.2946130.
- [35] D. Chen, L. Xiao, W. Yan, and Y. Guo, "A novel hybrid equivalent circuit model for lithium-ion battery considering nonlinear capacity effects," *Energy Reports*, vol. 7, pp. 320–329, 2021, doi: 10.1016/j.egy.2021.06.051.
- [36] Z.-Y. Chen *et al.*, "Benign-to-malignant transition in external short circuiting of lithium-ion batteries," *Cell Reports Phys. Sci.*, vol. 3, no. 6, p. 100923, 2022, doi: 10.1016/j.xcrp.2022.100923.
- [37] H. Yang *et al.*, "Coordinated demand response of rail transit load and energy storage system considering driving comfort," *CSEE J. Power Energy Syst.*, vol. 6, no. 4, pp. 749–759, 2020, doi: 10.17775/CSEEJPES.2020.02590.
- [38] Y. Cui *et al.*, "A high-voltage and stable zinc-air battery enabled by dual-hydrophobic-induced proton shuttle shielding," *Joule*, vol. 6, no. 7, pp. 1617–1631, 2022, doi: 10.1016/j.joule.2022.05.019.
- [39] C. Vidal, P. Malysz, P. Kollmeyer, and A. Emadi, "Machine Learning Applied to Electrified Vehicle Battery State of Charge and State of Health Estimation: State-of-the-Art," *IEEE Access*, vol. 8, pp. 52796–52814, 2020, doi: 10.1109/ACCESS.2020.2980961.
- [40] T. Kim, A. Adhikaree, and R. Pandey, "Outlier Mining-Based Fault Diagnosis for Multicell Lithium-Ion Batteries Using a Low-Priced Microcontroller," pp. 3365–3369.
- [41] Z. Hussain *et al.*, "Construction of rechargeable bio-battery cells from electroactive antioxidants extracted from wasted vegetables," *Clean. Eng. Technol.*, vol. 5, p. 100342, 2021, doi: 10.1016/j.clet.2021.100342.
- [42] E. N. Malev and T. H. Papanachev, "Simulation model development for evaluation of battery parameters," *11th Natl. Conf. with Int. Particip. Electron. 2020 - Proc.*, pp. 23–26, 2020, doi: 10.1109/ELECTRONICA50406.2020.9305149.
- [43] C. G. Cho, Z. Jia, J. B. Ahn, and H. J. Ryoo, "Design of a 5.4 kJ/s three-phase resonant converter based on a lithium polymer battery," *IEEE Trans. Dielectr. Electr. Insul.*, vol. 26, no. 2, pp. 381–389, 2019, doi: 10.1109/TDEI.2018.007724.
- [44] R. Elakya, J. Seth, P. Ashritha, and R. Namith, "Smart parking system using IoT," *Int. J. Eng. Adv. Technol.*, vol. 9, no. 1, pp. 6091–6095, 2019, doi: 10.35940/ijeat.A1963.109119.
- [45] Y. Song, M. Park, M. Seo, and S. W. Kim, "Online state-of-charge estimation for lithium-ion batteries considering model inaccuracies under time-varying current conditions," *IEEE Access*, vol. 8, pp. 192419–192434, 2020, doi: 10.1109/ACCESS.2020.3032752.
- [46] F. Yang, X. Song, F. Xu, and K. L. Tsui, "State-of-Charge Estimation of Lithium-Ion Batteries via Long Short-Term Memory Network," *IEEE Access*, vol. 7, pp. 53792–53799, 2019, doi: 10.1109/ACCESS.2019.2912803.
- [47] J. B. Axén, H. Ekström, E. W. Zetterström, and G. Lindbergh, "Evaluation of hysteresis expressions in a lumped voltage prediction model of a NiMH battery system in stationary storage applications," *J. Energy Storage*, vol. 48, no. January, 2022, doi: 10.1016/j.est.2022.103985.
- [48] I. Ojer, A. Berrueta, J. Pascual, P. Sanchis, and A. Ursua, "Development of energy management strategies for the sizing of a fast charging station for electric buses," *Proc. - 2020 IEEE Int. Conf. Environ. Electr. Eng. 2020 IEEE Ind. Commer. Power Syst. Eur. EEEIC / I CPS Eur. 2020*, 2020, doi: 10.1109/EEEIC/ICPSEurope49358.2020.9160716.
- [49] M. Kim, K. Kim, and S. Han, "Reliable Online Parameter Identification of Li-Ion Batteries in Battery Management Systems Using the Condition Number of the Error Covariance Matrix," *IEEE Access*, vol. 8, pp. 189106–189114, 2020, doi: 10.1109/access.2020.3031500.
- [50] X. Liu *et al.*, "Online identification of power battery parameters for electric vehicles using a decoupling multiple forgetting factors recursive least squares method," *CSEE J. Power Energy Syst.*, vol. 6, no. 3, pp. 735–742, 2020, doi: 10.17775/CSEEJPES.2018.00960.
- [51] P. Venegas, D. Gómez, M. Arrinda, M. Oyarbide, H. Macicior, and A. Bermúdez, "Kalman filter and classical Preisach hysteresis model applied to the state of charge battery estimation," *Comput. Math. with Appl.*, vol. 118, no. May, pp. 74–84, 2022, doi: 10.1016/j.camwa.2022.05.009.
- [52] R. Rai, M. Gaglani, S. Das, and T. Panigrahi, "Multi-Level Constant Current Based Fast Li-Ion Battery Charging Scheme with LMS Based Online State of Charge Estimation," *2020 IEEE Kansas Power Energy Conf. KPEC 2020*, pp. 1–6, 2020, doi: 10.1109/KPEC47870.2020.9167541.
- [53] Z. Huang, F. Yang, F. Xu, X. Song, and K. L. Tsui, "Convolutional Gated Recurrent Unit-Recurrent Neural Network for State-of-Charge Estimation of Lithium-Ion Batteries," *IEEE Access*, vol. 7, pp. 93139–93149, 2019, doi: 10.1109/ACCESS.2019.2928037.

- [54] M. Hossain, S. Saha, M. T. Arif, A. M. T. Oo, N. Mendis, and M. E. Haque, "A Parameter Extraction Method for the Li-Ion Batteries with Wide-Range Temperature Compensation," *IEEE Trans. Ind. Appl.*, vol. 56, no. 5, pp. 5625–5636, 2020, doi: 10.1109/TIA.2020.3011385.
- [55] D. M. Rosewater, D. A. Copp, T. A. Nguyen, R. H. Byrne, and S. Santoso, "Battery Energy Storage Models for Optimal Control," *IEEE Access*, vol. 7, pp. 178357–178391, 2019, doi: 10.1109/ACCESS.2019.2957698.
- [56] G. E. Mejia-ruiz, M. R. Arrieta, F. Rafael, S. Sevilla, and P. Korba, "Fast hierarchical coordinated controller for distributed battery energy storage systems to mitigate voltage and frequency deviations," *Appl. Energy*, vol. 323, no. May, p. 119622, 2022, doi: 10.1016/j.apenergy.2022.119622.
- [57] M. Schmid and C. Endisch, "Online diagnosis of soft internal short circuits in series-connected battery packs using modified kernel principal component analysis," *J. Energy Storage*, vol. 53, no. May, p. 104815, 2022, doi: 10.1016/j.est.2022.104815.
- [58] R. Hasan and J. Scott, "Extending Randles's Battery Model to Predict Impedance, Charge-Voltage, and Runtime Characteristics," *IEEE Access*, vol. 8, pp. 85321–85328, 2020, doi: 10.1109/ACCESS.2020.2992771.
- [59] H. Ben Sassi, F. Errahimi, N. Es-Sbai, and C. Alaoui, "Comparative study of ANN/KF for on-board SOC estimation for vehicular applications," *J. Energy Storage*, vol. 25, Oct. 2019, doi: 10.1016/j.est.2019.100822.
- [60] Li-Qing, G. Z. Jie, Chen-Hao, and He-Shuai, "High Precision Voltage Monitoring Technology for Multi-cell Battery Management System," *2020 IEEE 15th Int. Conf. Solid-State Integr. Circuit Technol. ICSICT 2020 - Proc.*, pp. 2020–2022, 2020, doi: 10.1109/ICSICT49897.2020.9278338.
- [61] T. G. T. A. Bandara, D. Ansean, J. C. Viera, L. Sanchez, and M. Gonzalez, "Fast charging protocols based on pulse-modulation with varying relaxation for electric vehicle li-ion cells," *2020 IEEE Veh. Power Propuls. Conf. VPPC 2020 - Proc.*, pp. 1–6, 2020, doi: 10.1109/VPPC49601.2020.9330917.
- [62] R. Hemmati and H. Mehrjerdi, "Stochastic linear programming for optimal planning of battery storage systems under unbalanced-uncertain conditions," *J. Mod. Power Syst. Clean Energy*, vol. 8, no. 5, pp. 971–980, 2020, doi: 10.35833/MPCE.2019.000324.
- [63] P. K. D. Pramanik *et al.*, "Power Consumption Analysis, Measurement, Management, and Issues: A State-of-the-Art Review of Smartphone Battery and Energy Usage," *IEEE Access*, vol. 7, pp. 182113–182172, 2019, doi: 10.1109/ACCESS.2019.2958684.